



# Microstructure and tribological properties of GLC/MoS<sub>2</sub> composite films deposited by magnetron sputtering

Xin Wang, Tao Wang, Man Ye, Li Wang, Guojun Zhang\*

School of Materials Science & Engineering, Xi'an University of Technology, Xi'an 710048, PR China

## ARTICLE INFO

### Keywords:

GLC/MoS<sub>2</sub> composite film  
Microstructure  
Tribological properties

## ABSTRACT

Graphite-like carbon (denoted as GLC)/MoS<sub>2</sub> composite films were deposited by closed field unbalanced magnetron sputtering system under different MoS<sub>2</sub> target currents. The microstructure of the films was investigated by means of X-ray diffraction (XRD) analysis, transmission electron microscopy (TEM) and X-ray photoelectron spectroscopy (XPS). The tribological behavior of GLC/MoS<sub>2</sub> composite films was evaluated using a ball-on-disk tribometer. The results revealed that with the increasing of MoS<sub>2</sub> target currents, the existing state of Cr from nanocrystallite to amorphous, leading to the lower of hardness. The film deposited at 0.4A MoS<sub>2</sub> target current exhibits the highest hardness (14.6 GPa) and elastic modulus (163.4 GPa) due to the structure of nanocrystallites embedded in amorphous matrix. Additionally, the film showed the lowest friction coefficient (about 0.1) and wear rate of  $1.3 \times 10^{-163} \text{ m}^3/\text{N}\cdot\text{m}$  under 30% RH as the MoS<sub>2</sub> target current increased to 1.6A. By contrast, the values of friction coefficient of other films were more than 0.2. On the other hand, the value of the friction coefficient of GLC/MoS<sub>2</sub> film decreased to 0.15 as MoS<sub>2</sub> target currents increased to 1.6A in the environment of much greater humidity (80% RH). These findings corroborate a thesis that the incorporation of GLC can improve the tribological properties of MoS<sub>2</sub> films in humid air environment.

## 1. Introduction

MoS<sub>2</sub> films have been widely used in the aerospace industry owing to their excellent tribological properties in high vacuum environment [1,2]. However, the tribological properties of pure MoS<sub>2</sub> film become worse in humid air environment due to its loose structure, high chemical activity to oxygen and hygroscopicity property [3,4]. These disadvantages restrict the application of MoS<sub>2</sub> film. Therefore, the transition metal elements (such as, for example, Ti or W or Cr) were added to optimize the performance of MoS<sub>2</sub> film in low and high humidity air [5]. Among the MoS<sub>2</sub>-Me films, MoS<sub>2</sub> doped with Ti films have been applied in industry due to their good tribological properties in ambient atmosphere [6–8]. However, doping Ti is useless to low friction in humid air environment.

The amorphous carbon films can be divided into graphite-like carbon (GLC) films and diamond-like carbon (DLC) films according to the main binding framework of sp<sup>2</sup> and sp<sup>3</sup> hybridization. GLC and DLC are dominated by sp<sup>2</sup> and sp<sup>3</sup> hybridization, respectively [9]. Recent studies reported that the addition of nonmetallic element C to MoS<sub>2</sub> film could improve the tribological performance of the film in air and humid environment [10–12]. As reported by Pimentel et al. [13], with increasing the carbon content, the friction coefficients of the Mo-S-C

composite coatings decreased from 0.2 to 0.04 in humid air. Similarly, Niakan et al. [11] found that the DLC-MoS<sub>2</sub> composite coatings prepared at low bias voltage exhibited lower friction coefficients in air environment. The DLC film has attracted great interest due to the high hardness and mechanical strength and excellent friction and wear performance [14]. Nevertheless, few study concerning the GLC/MoS<sub>2</sub> composite films. Previous researchers [15–18] have demonstrated that the GLC films had high hardness, low internal stress and excellent tribological performance in water and ambient atmosphere. In addition, another research has found that Cr doped GLC (graphite-like carbon) film exhibited high load bearing capacity as well as low friction in water, oil and ambient atmosphere [15]. Moreover, Cr interlayer could also improve the adhesion and load-bearing capacity of the films [19–21]. Thus, in order to prepare a film which has good tribological properties in both low and high humidity environments, the Cr, Ti doped GLC/MoS<sub>2</sub> composite films were deposited.

In this work, the GLC/MoS<sub>2</sub> composite films were prepared using magnetron sputtering techniques, and the microstructure and phase composition were characterized in detail. In addition, the effect of MoS<sub>2</sub> target current on microstructure, hardness, and friction coefficient in low and high humidity environments was systematically investigated.

\* Corresponding author.

E-mail address: [zhangguojun@xaut.edu.cn](mailto:zhangguojun@xaut.edu.cn) (G. Zhang).

<sup>3</sup> correct display  $10^{-16}$

**Table 1**  
Thickness and wear rate of GLC/MoS<sub>2</sub> films.

Sample ID	MoS <sub>2</sub> target current (A)	Composition (at.%)					Deposition time (min)	Film thickness (μm)	Wear rate (10 <sup>-15</sup> m <sup>3</sup> /N·m)
		Mo	S	C	Ti	Cr			
MS-0.4	0.4	15.21	20.83	30.21	7.95	25.80	175	1.87	0.98
MS-0.8	0.8	32.83	28.30	23.69	3.26	11.92	175	2.73	1.20
MS-1.2	1.2	35.75	39.02	14.83	2.51	7.89	175	3.71	3.14
MS-1.6	1.6	35.95	41.66	14.47	2.20	5.72	175	4.85	0.13

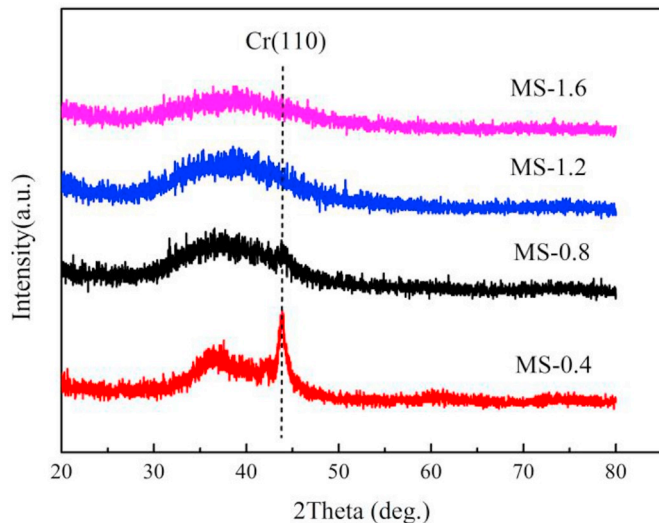


Fig. 1. XRD patterns of GLC/MoS<sub>2</sub> composite films.

## 2. Experimental

GLC/MoS<sub>2</sub> composite films deposited at different MoS<sub>2</sub> target currents were deposited on Si (100) wafers and stainless steel substrates by closed field unbalanced magnetron sputtering technique in argon (Ar) atmosphere. Four cathode targets, MoS<sub>2</sub> target (99.9% purity) and graphite target (99.99% purity), Ti target (99.99% purity) and Cr target (99.9% purity) were mounted in the vacuum chamber in a manner to form a closed magnetic field. Before deposition, the substrates were ultrasonically cleaned in acetone and ethanol bathes for 15 min respectively. Then the substrates were mounted on a rotated sample holder which was placed in the center of the vacuum chamber. When the base pressure was less than  $3 \times 10^{-34}$  Pa, Ar gas was introduced into the chamber with a flow rate of 20 sccm and the substrates were cleaned in glow discharge in Ar atmosphere under a bias voltage of -400 V. At first, a Cr adhesion layer 300 nm thick was pre-deposited on the substrates surface with the target current of 2.5A. And then, the transition layer was deposited by gradually increasing target current of MoS<sub>2</sub> to setting value (0.4A, 0.8A, 1.2A, 1.6A) and the current of graphite target and Ti target to 2.5 A and 0.3A, respectively. Simultaneously the current of the Cr target was decreasing to 0.2 A. Finally, by changing the currents of MoS<sub>2</sub> target, the GLC/MoS<sub>2</sub> composite films were deposited. During the deposition process, the rotation rate of the sample holder was 5 rad/min and the bias voltage for the deposition of the films was -60 V. Other deposition parameters are listed in Table 1.

The crystallinity and phase structures of GLC/MoS<sub>2</sub> films were analyzed using X-ray diffraction (XRD). The scanning range from 20° to 80° with a speed of 10°/min. The chemical bonds and composition of the GLC/MoS<sub>2</sub> films were analyzed by X-ray photoelectron

spectroscopy (XPS, K-Alpha). Before testing, the sample surface was etched in argon atmosphere to remove contaminants. The crystal structure and microstructure of GLC/MoS<sub>2</sub> films were studied by high resolution transmission electron microscopy (HRTEM). The preparation process of cross-sectional specimens for TEM observation comprises the following procedures. First, the films deposited on Si wafer substrates was cut into two small pieces and adhered face-to-face, and then let the thickness of the specimen less than 20 μm using mechanical polishing. Finally, to obtained composite area, the specimens were bombarded by Ar ion beam. Based on the Oliver-Pharr method [22], the hardness and elastic modulus of GLC/MoS<sub>2</sub> films were evaluated by nanoindentation test using a Berkovich indenter in Agilent Nano-indenter G200. To eliminate the effects of substrate deformation, the indentation depth of 200 nm was controlled less than 10% of the film thickness. The tribological performances of GLC/MoS<sub>2</sub> films in low and high humidity environments were tested by ball-on-disk tribometer at room temperature. The GCr15 ball with a diameter of 5 mm was used as sliding counterpart. Applied load was kept at 2 N with a sliding speed at 300 mm/s, the sliding time was 2250 s. The specific wear rate was calculated by the equation [23]:  $K = V / SF$ , where V is the wear volume in m<sup>3</sup>, S is the total sliding distance in meters and F is the applied load in newtons. Wear volume V was determined by integrating the cross-sectional profile of the wear track which was profiled by the LEXT OLS 4000 Laser Measuring Microscope.

## 3. Results and discussion

### 3.1. Microstructure and mechanical properties

The X-ray diffraction patterns of GLC/MoS<sub>2</sub> composite films deposited at different MoS<sub>2</sub> target currents are presented in Fig. 1. As seen from Fig. 1, a diffraction peak of MS-0.4 film observed at the angle around 44° can correspond to (110) of Cr phase. When the currents of MoS<sub>2</sub> target were higher than 0.8A, the intensity of Cr (110) diffraction peak disappears and only Boultin-peaks presented in the XRD pattern. It indicates that the film deposited at 0.4A MoS<sub>2</sub> target current exhibiting the structure of Cr nanocrystallites embedded in amorphous C and MoS<sub>2</sub> matrix, when the currents of MoS<sub>2</sub> target increased to 0.8A, a prevailing part of the structure of GLC/MoS<sub>2</sub> composite films was amorphous.

Fig. 2 shows the cross-sectional TEM and HRTEM micrographs of deposited GLC/MoS<sub>2</sub> composite films on Si substrate, Figs. b and d are enlarged views of Figs. a and c, respectively. For the sample of MS-0.4, as seen from Fig. 2a, bright rings were observed in the corresponding selected area electron diffraction image (SAED), which was identified as Cr. In HRTEM image (Fig. 2b), Cr nanocrystallites are embedded in the MoS<sub>2</sub> and C matrix. As MoS<sub>2</sub> target exceeding 0.8A, nanocrystallites were not found of the GLC/MoS<sub>2</sub> composite films in the Fig. 2c, e and f, and their corresponding SAED patterns showed broad and diffuse diffraction halo, which indicated that the GLC/MoS<sub>2</sub> composite film was amorphous. Additionally, multilayer structure of the rich MoS<sub>2</sub> layer and the rich GLC layer was formed in the composite films because of the rotation of sample holder in the process of deposition. Those results illustrate that the high MoS<sub>2</sub> target current affects the

<sup>a</sup> correct display 10<sup>-3</sup>

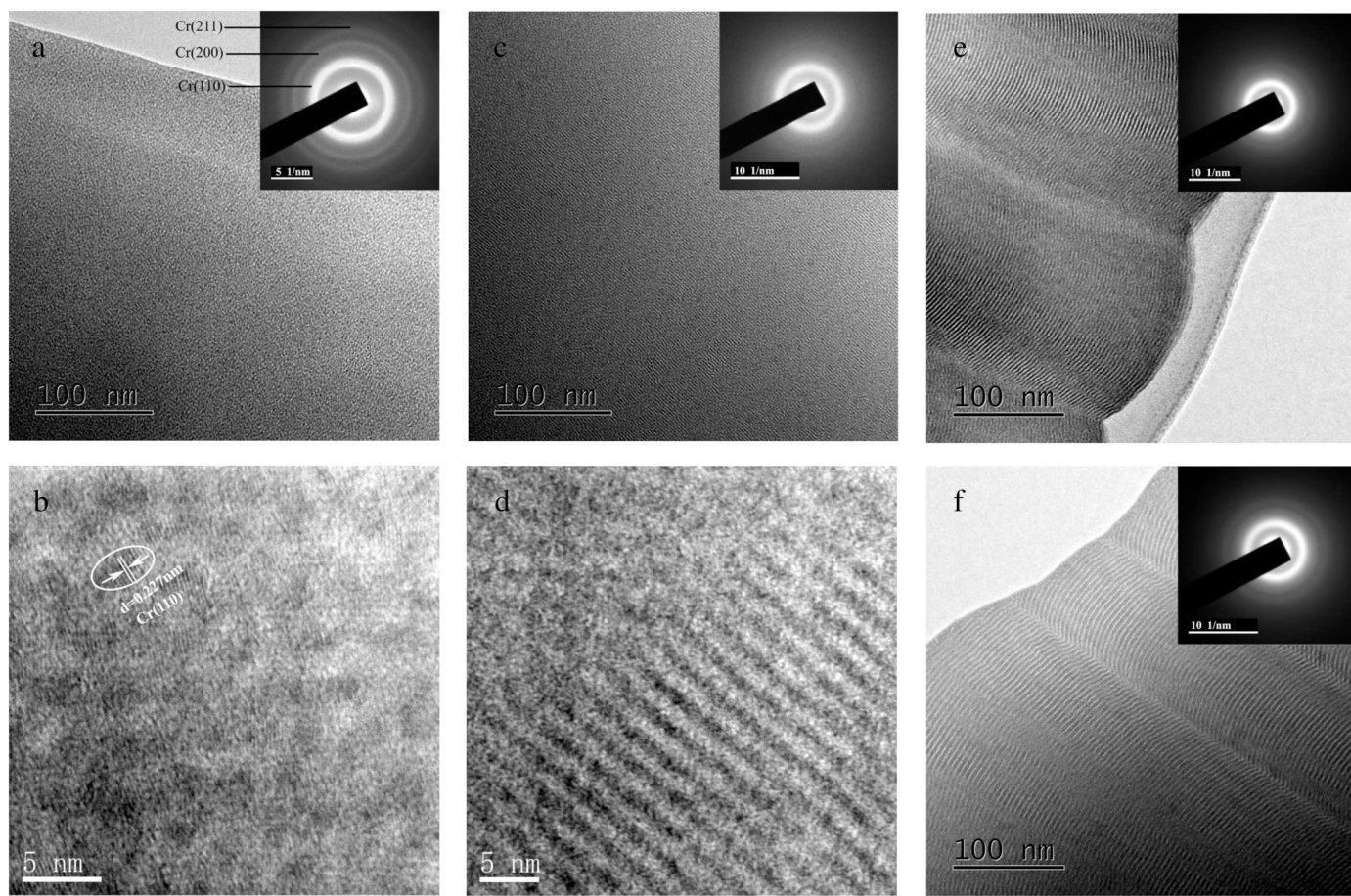


**Fig. 2.** Cross-sectional TEM and HRTEM images of GLC/MoS<sub>2</sub> composite films and their corresponding SAED: (a), (b) MS-0.4, (c), (d) MS-0.8, (e) MS-1.2 and (f) MS-1.6.

existing state of Cr from nanocrystallite to amorphous, which was in agreement with the results of the XRD.

The chemical bonds of the GLC/MoS<sub>2</sub> composite film deposited at 0.4A and 1.6A MoS<sub>2</sub> target currents were characterized by XPS. As seen from Fig. 3, the C 1s, Mo 3d, S 2p, Cr 2p and Ti 2p spectrum of the MS-0.4 and MS-1.6A film are fitted by Gaussian-Lorentzian function. The C 1s spectrum of the MS-0.4 and MS-1.6A film can be decomposed into two peaks. The peaks corresponded to the C=C bond (284.4 eV) and C-C bond (285.4 eV) [24]. Therefore, it can be concluded that the composite films are dominated by sp<sup>2</sup> hybridization of C atoms with

the characteristic of graphite-like C atoms arrangements. As shown in Fig. 3(c) and (d), the peaks of the Mo 3d spectrum at around 229.22 eV and 232.30 eV are identified as MoS<sub>2</sub> and the peaks at 228.34 eV and 231.50 eV are assigned to MoS [24]. The Mo 3d spectrum also shows a small peak at 226.12 eV binding energy, which is identified as the peak of S 2s [13]. The S 2p spectrum (Fig. 3e–f) exhibits double peaks at 162.28 eV and 163.4 eV, which represents the S<sup>2-</sup> in MoS<sub>2</sub>. However, another double peaks are encountered in this spectrum as well, which are assigned to MoS (161.62 eV and 162.8 eV). Therefore, both MoS<sub>2</sub> and MoS exist in the composite films. As shown in Fig. 3(g) and



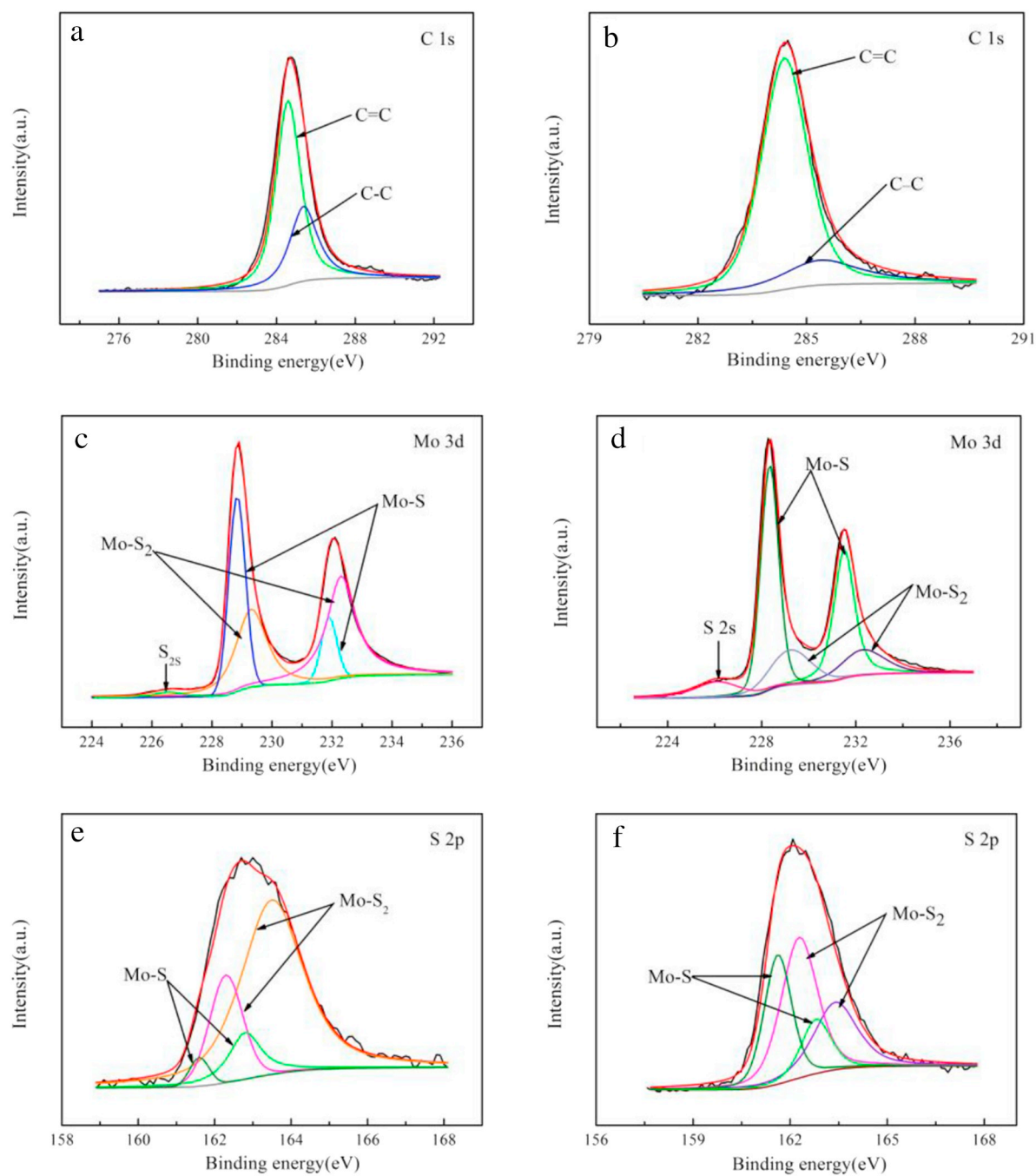


Fig. 3. XPS spectra of GLC/MoS<sub>2</sub> composite film: (a), (c), (e), (g), (i) MS-0.4, (b), (d), (f), (h), (j) MS-1.6.

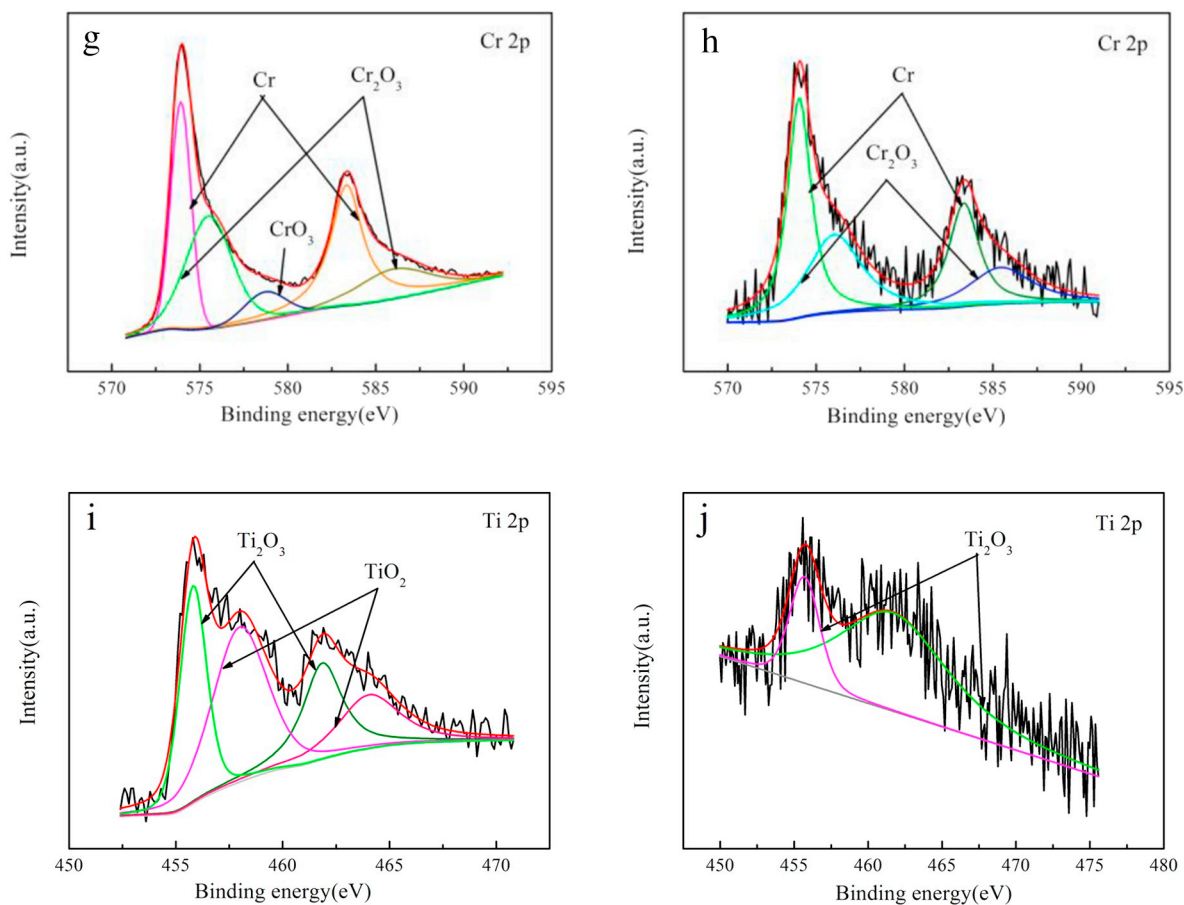
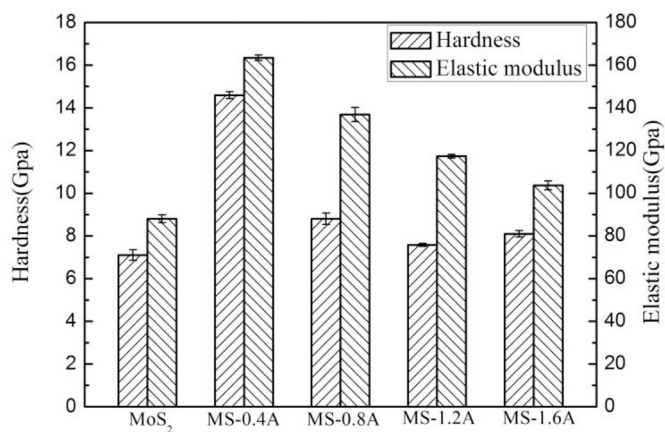


Fig. 3. (continued)

Fig. 4. Hardness and elastic modulus of the GLC/MoS<sub>2</sub> composite films.

(h), the peaks of the Cr 2p spectrum at around 573.9 eV and 583.4 eV can be ascribed to metallic Cr, and the peaks at around 575.9 eV and 586.1 eV are assigned to Cr<sub>2</sub>O<sub>3</sub>, and the peak at around 578.9 eV is identified as CrO<sub>3</sub>. Fig. 3(h) shows the Cr 2p peaks of Cr–Cr (binding energy 574.1 and 583.5 eV) and Cr–O (binding energy 576.1 and 586.1 eV). The Ti 2p spectrum is shown in Fig. 3(i) and (j), and in Fig. 3(i) the peaks at around 455.8 eV and 461.8 eV are assigned to Ti<sub>2</sub>O<sub>3</sub>, and the peaks at around 458.2 eV and 464.3 eV are identified as TiO<sub>2</sub>. In Fig. 3(j), the peaks at around 455.6 eV and 461.6 eV are assigned to Ti<sub>2</sub>O<sub>3</sub>.

Fig. 4 shows the hardness and elastic modulus of the GLC/MoS<sub>2</sub> composite films. One can see that, the hardness of the GLC/MoS<sub>2</sub> composite films varies from 7.6 to 14.6 GPa. And it is much higher than that results of Gu Lei and J.V. Pimentel et al. [12,13]. And the hardness of GLC/MoS<sub>2</sub> composite films is higher than pure MoS<sub>2</sub> film. MS-0.4 with 0.4A MoS<sub>2</sub> target current shows the highest hardness (14.6 GPa) and elastic modulus (163.4 GPa). When the currents of MoS<sub>2</sub> target increased from 0.8A to 1.6A, the hardness of GLC/MoS<sub>2</sub>

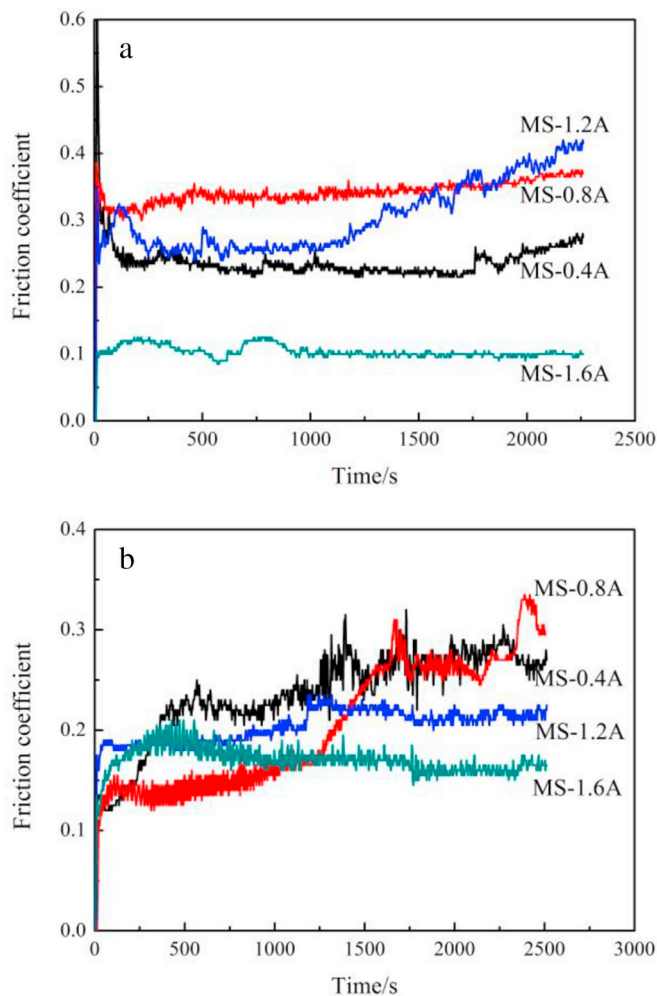


Fig. 5. Friction coefficients of the GLC/MoS<sub>2</sub> composite films in low and high humidity environments: (a) 30% RH in air and (b) 80%RH in air.

composite films changes slightly. The high hardness of MS-0.4 was mainly due to its different microstructure, plausibly due to Cr nanocrystallites.

### 3.2. Tribological properties

Friction tests of as-deposited films were carried out in air for 30% RH and 80%RH, respectively. Fig. 5 presents the friction curves of the GLC/MoS<sub>2</sub> composite films in low and high humidity environments under an applied load of 2 N. As seen from Fig. 5(a), MS-1.6 film exhibits stable and the lowest friction coefficient (around 0.1) during the whole testing process and the friction coefficient of other films were larger than 0.2. The MS-0.4 film showed low and stable COF  $\sim$ 0.2. But the friction coefficient of MS-1.2 film maintained the relative steady state at the early stage of sliding and rose suddenly after approximately 1000 s. It can be concluded that, with the increase of MoS<sub>2</sub> target currents, the amorphous MoS<sub>2</sub> serve as solid lubricant during the tribological test. In addition the suitable addition of Ti, Cr and GLC improved the tribological behavior of the films under ambient atmosphere [12,26]. Meanwhile, high hardness had contributed to improving the tribological properties of MS-0.4 film [25,27]. As seen from Fig. 5(b), the friction coefficient of GLC/MoS<sub>2</sub> films decreases as MoS<sub>2</sub> target current increased. And the MoS<sub>2</sub> target current increased to 1.6A, the film exhibited the lowest friction coefficient (about 0.15). The friction coefficient of other films were also larger

than 0.2. But the friction coefficient of other films in high humidity environment was lower than that in low humidity environment. It indicated that the GLC/MoS<sub>2</sub> composite films were less sensitive to water vapor during tribological testing and that MS-1.6 coating has excellent tribological properties both at low and high relative humidity environment.

In order to revealing the wear mechanisms of the GLC/MoS<sub>2</sub> composite films, a comparison of wear scar and corresponding curves of the GLC/MoS<sub>2</sub> composite films in air with 30% relative humidity were carried out. Fig. 6 presents the wear scars of the films under applied load of 2 N.

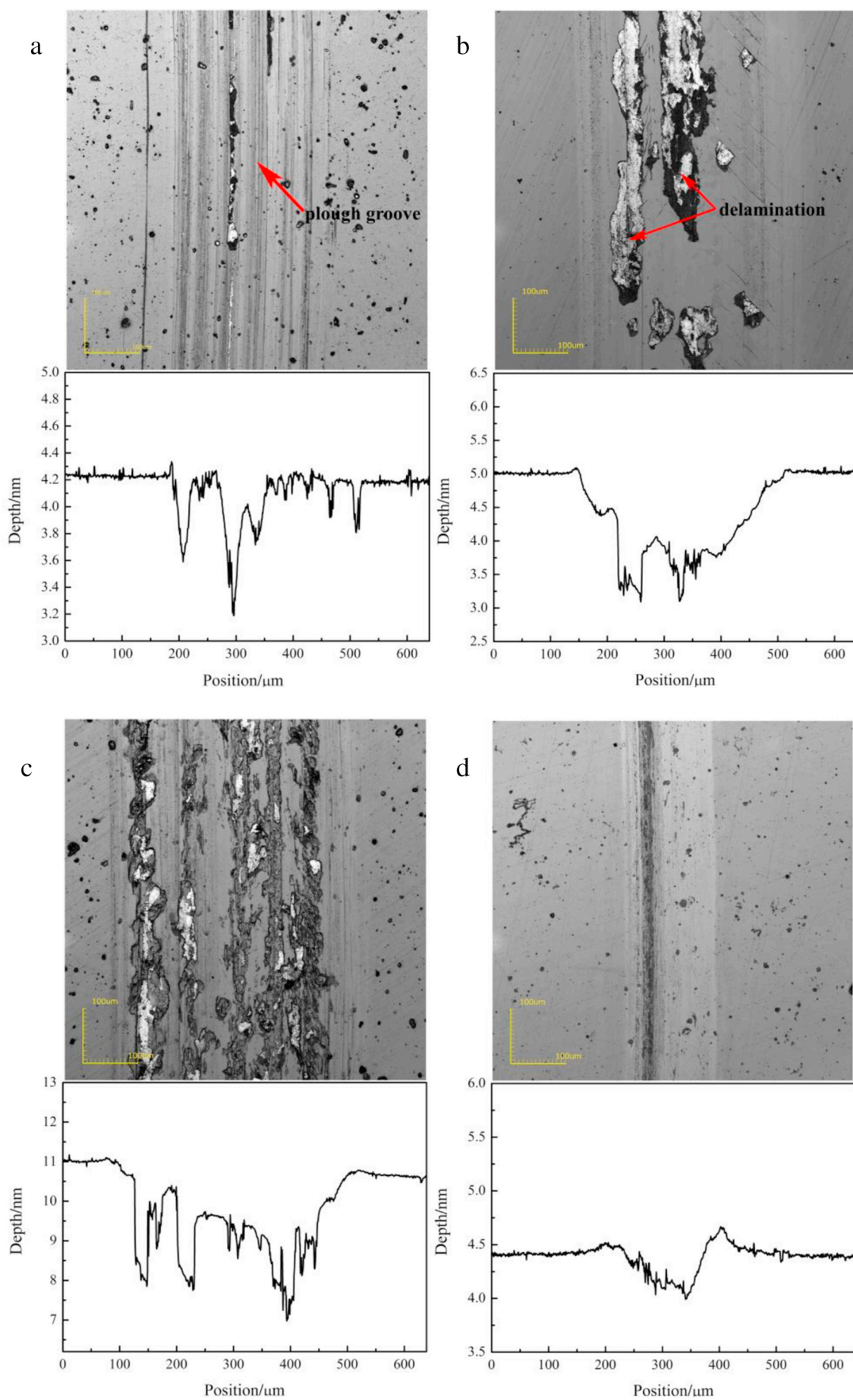
The wear scars mainly contain plough grooves and local fatigue delamination which revealed that the wear of the films might due to micro-plough and delamination. Clearly, the plough grooves are narrow and shallow, while the delamination is wide and deep. Thus it can be proposed that the delamination is the main reason of the composite coatings failure. It should be noted that MS-1.6 exhibited smooth and narrow wear track, while the wear track of MS-0.8 and MS-1.2 showed a distinct black region, that is to say pieces of films peeled off from the substrates. The wear scar of MS-0.4 was mainly plough grooves, which were narrow and deep. The low friction coefficient corresponded to wear scars which were narrow and shallow.

The wear rate of the composite films under low humidity (30% RH) was shown in Table 1. The results suggested that the value of wear rate of the GLC/MoS<sub>2</sub> composite films was of the order of  $10^{-6}$  mm<sup>3</sup>/Nm. Among these samples, the MS-1.6 showed the better wear resistance. Compared with the conventional MoS<sub>2</sub>-based films, the GLC/MoS<sub>2</sub> composite films are less sensitive to moisture. For example, MoS<sub>2</sub>-Ti composite films had excellent wear resistant in atmosphere environment, while that resistance was unsatisfactory when sliding in high humid environment [28], and some films were still suffered from the structural degradation and poor coating adhesion to substrate. Normally, the intrinsic solid lubricant GLC films exhibit lower COF and show less sensitive to high humidity. The improved tribological properties of GLC/MoS<sub>2</sub> composite films might be attributed to the addition of GLC. Meanwhile, the hardness of as-deposited GLC/MoS<sub>2</sub> composite films (7.6–14.6 GPa) was higher than MoS<sub>2</sub>-Ti films (5.21–9.69 GPa) and MoS<sub>2</sub>-C films (7.0–10.8 GPa) [12].

### 4. Conclusions

GLC/MoS<sub>2</sub> composite films were deposited by closed field unbalanced magnetron sputtering system at different MoS<sub>2</sub> target currents. The GLC/MoS<sub>2</sub> composite film deposited at 0.4A MoS<sub>2</sub> target current exhibited the structure of Cr nanocrystallines embedded in amorphous C and MoS<sub>2</sub> matrix. Meanwhile, it showed the highest hardness (14.6 GPa) and elastic modulus (163.4 GPa). When the currents of MoS<sub>2</sub> target increased up to 0.8A, the structure of the films gradually transferred into amorphous and the hardness decreased obviously. The tribological performance of GLC/MoS<sub>2</sub> composite films was tested in environments of low humidity (30% RH) and high humidity (80% RH). The results showed that when the MoS<sub>2</sub> target current increased to 1.6A, the GLC/MoS<sub>2</sub> composite film exhibited low friction coefficient (about 0.1), low wear rate and greater resistance to wear in atmosphere environment with 30% RH. Meanwhile, the low friction coefficient was also found in high humidity (about 0.15). Those results proved that the GLC/MoS<sub>2</sub> composite films hold great potential to be used in multiple environments as a protective film.

<sup>2</sup> Correct display  $10^{-6}$



(caption on next page)



Fig. 6. Wear scar and corresponding curves of the GLC/MoS<sub>2</sub> composite films: (a) MS-0.4, (b) MS-0.8, (c) MS-1.2 and (d) MS-1.6.

## Acknowledgements

This subject was supported by the National Natural Science Foundation of China (Grant Nos. 51601144, 51674196 and 51371141).

## References

- [1] C. Donnet, A. Erdemir, Solid lubricant coatings: recent developments and future trends, *Tribol. Lett.* 17 (2004) 389–397.
- [2] P.D. Fleischauer, J.R. Lince, A comparison of oxidation and oxygen substitution in MoS<sub>2</sub> solid film lubricants, *Tribol. Int.* 32 (1999) 627–636.
- [3] N.M. Renevier, J. Hampshire, V.C. Fox, J. Witts, T. Allen, D.G. Teer, Advantages of using self-lubricating, hard, wear-resistant MoS<sub>2</sub>-based coatings, *Surf. Coat. Technol.* 142 (2001) 67–77.
- [4] X.Z. Ding, X.T. Zeng, X.Y. He, Z. Chen, Tribological properties of Cr- and Ti-doped MoS<sub>2</sub> composite coatings under different humidity atmosphere, *Surf. Coat. Technol.* 205 (2010) 224–231.
- [5] M.C. Simmonds, A. Savan, E. Pflüger, H. Van Swygenhoven, Mechanical and tribological performance of MoS<sub>2</sub> co-sputtered composites, *Surf. Coat. Technol.* 126 (2000) 15–24.
- [6] F. Bülbül, İhsan. Efeoglu, MoS<sub>2</sub>-Ti composite films having (002) orientation and low Ti content, *Crystallogr. Rep.* 55 (2010) 1177–1182.
- [7] S.M. Aouadi, Y. Paudel, B. Luster, S. Stadler, P. Kohli, C. Muratore, C. Hager, A.A. Voevodin, Adaptive Mo<sub>2</sub>N/MoS<sub>2</sub>/Ag tribological nanocomposite coatings for aerospace applications, *Tribol. Lett.* 29 (2008) 95–103.
- [8] D.G. Teer, J. Hampshire, V. Fox, V. Bellido-Gonzalez, The tribological properties of MoS<sub>2</sub>/metal composite coatings deposited by closed field magnetron sputtering, *Surf. Coat. Technol.* 94–5 (1997) 572–577.
- [9] Paul K. Chu, Liuhe Li, Characterization of amorphous and nanocrystalline carbon films, *Mater. Chem. Phys.* 96 (2006) 253–277.
- [10] T. Polcar, A. Cavaleiro, Review on self-lubricant transition metal dichalcogenide nanocomposite coatings alloyed with carbon, *Surf. Coat. Technol.* 206 (2011) 686–695.
- [11] H. Niakan, C. Zhang, L. Yang, Q. Yang, J.A. Szpunar, Structure and properties of DLC–MoS<sub>2</sub> composite films synthesized by BTBD method, *J. Phys. Chem. Solids* 75 (2014) 1289–1294.
- [12] Gu Lei, Peiling Ke, Yousheng, Zou Xiaowei, et al., Amorphous self-lubricant MoS<sub>2</sub>-C sputtered coating with high hardness, *Appl. Surf. Sci.* 331 (2015) 66–71.
- [13] J.V. Pimentel, T. Polcar, A. Cavaleiro, Structural, mechanical and tribological properties of Mo-S-C solid lubricant coating, *Surf. Coat. Technol.* 205 (2011) 3274–3279.
- [14] Li Ji, Hongxuan Li, Fei Zhao, Weilong Quan, Jianmin Chen, Huidi Zhou, Atomic oxygen resistant behaviors of Mo/diamond-like carbon nanocomposite lubricating films, *Appl. Surf. Sci.* 255 (2009) 4180–4184.
- [15] J. Stallard, D. Mercs, M. Jarratt, D.G. Teer, P.H. Shipway, A study of the tribological behaviour of three carbon-based coatings, tested in air, water and oil environments at high loads, *Surf. Coat. Technol.* 177–178 (2004) 545–551.
- [16] Fei Zhou, Xiaolei Wang, Koji Kato, Zhendong Dai, Friction and wear property of a-CN<sub>x</sub> coatings sliding against Si<sub>3</sub>N<sub>4</sub> balls in water, *Wear* 263 (2007) 1253–1258.
- [17] H. Huang, X. Wang, J. He, Synthesis and properties of graphite-like carbon by ion beam-assisted deposition, *Mater. Lett.* 57 (2003) 3431–3436.
- [18] S.K. Field, M. Jarratt, D.G. Teer, Tribological properties of graphite-like and diamond-like carbon coatings, *Tribol. Int.* 37 (2004) 949–956.
- [19] C. Wei, J.-Y. Yen, Effect of film thickness and interlayer on the adhesion strength of diamond like carbon films on different substrates, *Diam. Relat. Mater.* 16 (2007) 1325–1330.
- [20] Y.S. Li, Y. Tang, Q. Yang, C. Xiao, A. Hirose, Growth and adhesion failure of diamond thin films deposited on stainless steel with ultra-thin dual metal interlayers, *Appl. Surf. Sci.* 256 (2010) 7653–7657.
- [21] G. Capote, L.F. Bonetti, L.V. Santos, V.J. Trava-Airoldi, E.J. Corat, Adherent amorphous hydrogenated carbon films on metals deposited by plasma enhanced chemical vapor deposition, *Thin Solid Films* 516 (2008) 4011–4017.
- [22] Q. Kan, W. Yan, G. Kang, Q. Sun, Oliver-Pharr indentation method in determining elastic moduli of shape memory alloys—a phase transformable material, *J. Mech. Phys. Solids* 61 (2013) 2015–2033.
- [23] Yongxin Wang, Jinlong Li, Lei Shan, Jianmin Chen, Qunji Xue, Tribological performances of the graphite-like carbon films deposited with different target powers in ambient air and distilled water, *Tribol. Int.* 73 (2014) 17–24.
- [24] Xiaopeng Qin, Peiling Ke, Aiyang Wang, Kwang Ho Kim, Microstructure, mechanical and tribological behaviors of MoS<sub>2</sub>-Ti composite coatings deposited by a hybrid HIPIMS method, *Surf. Coat. Technol.* 228 (2013) 275–281.
- [25] E. Arslan, Y. Totik, I. Efeoglu, Comparison of structure and tribological properties of MoS<sub>2</sub>-Ti films deposited by biased-dc and pulsed-dc, *Prog. Org. Coat.* 74 (2012) 772–776.
- [26] Y. Wang, L. Wang, Q. Xue, Controlling wear failure of graphite-like carbon film in aqueous environment: two feasible approaches, *Appl. Surf. Sci.* 257 (2011) 4370–4376.
- [27] Meidong Huang, Xueqian Zhang, Peiling Ke, Aiyang Wang, Graphite-like carbon films by high power impulse magnetron sputtering, *Appl. Surf. Sci.* 283 (2013) 321–326.
- [28] X. Zhang, R.G. Vitchev, W. Lauwerens, L. Stals, J. He, J.P. Celis, Effect of crystallographic orientation on fretting wear behaviour of MoS<sub>x</sub> coatings in dry and humid air, *Composite Solid Films* 396 (2001) 69–77.